

## Image-potential-induced resonances at free-electron-like metal surfaces

S. Papadia, M. Persson, and L.-A. Salmi

*Institute of Theoretical Physics, Chalmers University of Technology, S-412 96 Göteborg, Sweden*

(Received 9 March 1990)

The formation of electronic image states at free-electron-like metal surfaces is described with a jellium model where the lattice-induced corrugation is included via a pseudopotential description. Comparison with inverse-photoemission experiments on Al(111) gives good agreement between the calculated and the measured resonant state energy. Statements are made about the possible resolution of such resonances at other metal surfaces.

The analysis of the formation of electronic surface states on materials is an important part in the study of the physical and chemical properties of materials. Surface states can experimentally be observed by direct- and inverse-photoemission spectroscopy, and theoretically they can be identified in electronic-structure calculations.<sup>1-4</sup> The nearly-free-electron metals have a particularly simple electronic structure since the effects of the ion cores on the conduction electrons are well described by weak pseudopotentials. An example of such a metal is aluminium where observed surface states on Al(100) have been accounted for in surface electronic-structure calculations using pseudopotentials.<sup>5,6</sup> In this case, the surface-state formation can be understood in terms of a high substrate reflectivity for the electrons provided by a band gap in the metal.

In the presence of a free-electron-like overlayer, as in Na/Al(111), surface resonances have been observed by inverse photoemission in an energy region with no band gap.<sup>7</sup> In this case the required reflectivity for the resonance formation is provided by the sharp interface potential.<sup>8,9</sup> More surprising is the fact that a surface state has been observed close to the vacuum level, far from any metal band gap, on the surface of clean Al(111).<sup>7</sup> This state was interpreted as an image state—a resonant state that is associated with the asymptotic imagelike behavior of the surface-barrier potential and lies close to the vacuum level in energy. In the analysis, no mechanism was identified that could provide the necessary reflectivity for such a state to form in an energy region with no band gap.

In this Rapid Communication we present a model for image-state formation at free-electron-like metals and apply it explicitly to Al(111). We follow a multiple-reflection approach for surface-state formation where the substrate and barrier reflectivities are calculated within a jellium model and the lattice corrugation of the substrate is described with a pseudopotential. We find that the lattice-induced corrugation of aluminium's potential provides enough reflectivity for an image-potential-induced surface state to form on Al(111). The calculated energy position of the surface state, 0.47 eV below the vacuum level, is in good agreement with the observed energy of 0.54 eV below the vacuum level.<sup>7</sup> We also find favorable conditions for this kind of resonant state to be resolved on other nearly-free-electron metals such as Ba and Pb.

The induced density of states on the surface of Al(111)

is calculated in the following. Hartree atomic units are implicitly understood if not stated otherwise. In the multiple-reflection approach for surface-state formation<sup>10</sup> (cf. Fig. 1), electronic states are identified from the behavior of the total wave  $\Psi_{\text{tot}}$ . The total wave is formed by multiple reflection of the incident electron wave  $\Psi_{\text{inc}}$  back and forth between a crystal potential reference plane and a surface-barrier reference plane. Diffracted waves are neglected since their influence on the specular beam from the crystal is only a second-order effect. Within this approximation,  $\Psi_{\text{tot}}$  is given by

$$\Psi_{\text{tot}} = \left[ r^- + \frac{t^- t^+ r_B}{1 - r_B r_C} \right] \Psi_{\text{inc}}, \quad (1)$$

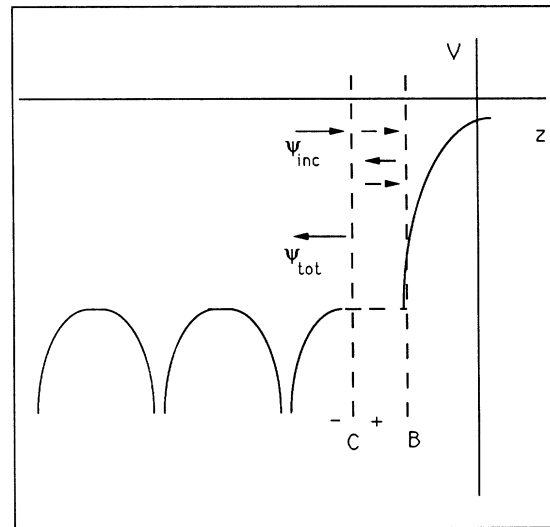


FIG. 1. Schematic picture of the multiple-scattering approach for surface-state formation. Electron waves are multiply reflected at the crystal potential reference plane (C) and at the surface-barrier reference plane (B). These reference planes are infinitesimally separated with a constant potential so that the electron waves propagate as plane waves between the planes. In our calculations, planes (C) and (B) are situated at the jellium edge, i.e., at half an interlayer's distance outside (towards the vacuum side of) the first lattice plane. An extra phase is picked up due to the definition of the first lattice plane as the scattering plane in Eq. (3).

where (cf. Fig. 1)  $r^-$  is the reflectance at the minus side of the reference plane  $C$ ,  $t^-$  and  $t^+$  are the transmittances at the minus and plus sides of plane  $C$ , respectively. The quantity  $r_C$  is the reflectance at the plus side of the crystal potential reference plane and  $r_B$  is the surface-barrier reflectance. The surface bound and resonant states occur at energies where  $\Psi_{\text{tot}}$  has a pole or where  $1 - r_B r_C$  has a minimum.

With the purpose of estimating the substrate reflectivity

$$G_+(r, r') = -\frac{i}{2} \int \frac{d^2 k_{\parallel}}{(2\pi)^2} \frac{\exp(i\mathbf{k}_{\perp} |z - z'|) \exp[i\mathbf{k}_{\parallel} \cdot (\mathbf{r}_{\parallel} - \mathbf{r}'_{\parallel})]}{|\mathbf{k}_{\perp}|}, \quad (2)$$

where  $\mathbf{k}_{\perp}$  and  $\mathbf{k}_{\parallel}$  denote the momentum components perpendicular and parallel to the surface, respectively, we arrive at the following result—in the Born approximation—for the amplitude  $r_C(\mathbf{k}, \mathbf{k}')$  of the elastically scattered wave:

$$r_C(\mathbf{k}, \mathbf{k}') = -i \frac{v(\mathbf{k}' - \mathbf{k})}{|\mathbf{a} \times \mathbf{b}| |\mathbf{k}_{\perp}| (1 - \exp[-i(\mathbf{k}'_{\perp} - \mathbf{k}_{\perp}) \cdot \mathbf{d}])}. \quad (3)$$

Here  $\mathbf{k}$  and  $\mathbf{k}'$  are the momenta of the incident and scattered wave, respectively. We also have that  $\mathbf{a}$  and  $\mathbf{b}$  are surface base vectors,  $\mathbf{d} = d\hat{\mathbf{z}}$  is the distance between crystal planes parallel to the surface, and  $v(\mathbf{k}' - \mathbf{k})$  is the Fourier transform of the pseudopotential in the unit cell. The surface periodicity gives the restriction that  $\mathbf{k}'_{\parallel} = \mathbf{k}_{\parallel} + \mathbf{g}_{\parallel}$ , where  $\mathbf{g}_{\parallel}$  is a surface reciprocal-lattice vector. We normalize  $\Psi_{\text{inc}}$  to unity and express  $\Psi_{\text{tot}}$ ,  $r_C$ , and  $r_B$  as  $e^{i\Phi_{\text{tot}}}$ ,  $|r_C| e^{i\Phi_C}$ , and  $|r_B| e^{i\Phi_B}$ , respectively. Using the fact that  $|r_B| = 1$  for a surface barrier, we arrive at an expression for the total wave  $\Psi_{\text{tot}} = e^{i\Phi_{\text{tot}}}$  as

$$e^{i\Phi_{\text{tot}}} = \frac{t^- t^+}{1 - |r_C|^2} e^{i\Phi_B} \left( \frac{1 - |r_C| e^{-i\tilde{\Phi}}}{1 - |r_C| e^{i\tilde{\Phi}}} \right), \quad (4)$$

where  $\tilde{\Phi}$  is equal to  $\Phi_C + \Phi_B$ . Note the unitary condition that  $|t^- t^+|$  is equal to  $1 - |r_C|^2$ .

The induced density of states is related to the variation of the total phase shift  $\Phi_{\text{tot}}$  with respect to energy.<sup>12</sup> The energy derivative of the term  $|t^- t^+|/(1 - |r_C|^2)$  in Eq. (4) is omitted because its variation is small compared to the strong variation of the barrier phase shift  $\Phi_B$  induced by the image part of the potential. The energy derivative of the total phase shift is then given by

$$\frac{\partial \Phi_{\text{tot}}}{\partial \varepsilon} = \frac{\partial \Phi_B}{\partial \varepsilon} + 2|r_C| \frac{\partial \tilde{\Phi}}{\partial \varepsilon} \left( \frac{\cos(\tilde{\Phi}) - |r_C|}{1 + |r_C|^2 - 2|r_C| \cos(\tilde{\Phi})} \right). \quad (5)$$

The induced density of states, related to  $\partial \Phi_{\text{tot}}/\partial \varepsilon$  which at the energy of interest gives by far the largest contribution, peaks at the resonant condition  $\Phi_C + \Phi_B = n2\pi$ , as can be seen in Eq. (5). The barrier phase shift  $\Phi_B$  has been calculated by numerical integration of the one-electron Schrödinger equation for a jellium model potential for Al. In this jellium model, the electron density parameter for aluminium  $r_s$  is chosen to be  $r_s = 2.07$  and the local-density approximation (LDA) is made for exchange and

$r_C$ , we calculate the scattering amplitude for a plane wave impinging on a semi-infinite crystal of Al(111). The substrate potential is modeled with a local, screened pseudopotential representation of the ions.<sup>11</sup> The pseudopotential parameters were originally fitted to the measured phonon dispersion curves of aluminium. Using the wave-vector representation of the (retarded) Green's function for the Helmholtz equation, given by

correlation effects. Since LDA results in an exponential behavior for the long-range part of the potential, we correct for the right imagelike behavior.<sup>13</sup> The phase shift due to the crystal potential  $\Phi_C$  is extracted from the specular scattering amplitude of electrons incident normal to the surface [ $r_C(\mathbf{k}, \mathbf{k}')$  in Eq. (3) with  $\mathbf{k}' = -\mathbf{k}_{\perp}$ ].

The energy derivative of the total phase shift versus energy for Al(111) is shown in Fig. 2 for three different crystal reflectivities. For  $|r_C| = 0$ , corresponding to no lattice effects on the potential, there is a smooth variation of  $\partial \Phi_{\text{tot}}/\partial \varepsilon$  with respect to energy, as noted by Lindgren and Walldén.<sup>14</sup> But already for  $|r_C| = 0.1$  we begin to see a resonance which becomes more pronounced with higher  $|r_C|$ . The value  $|r_C| = 0.1$  is what we obtain from Eq. (3) for Al(111) at an energy within 1 eV below the vacuum level. The barrier phase shift diverges at the level and, asymptotically, the width of the resonance (full width at half maximum) is, according to Eq. (5), given by  $2|r_C|^{-1/2} |\partial \tilde{\Phi}/\partial \varepsilon|^{-1}$  for small  $|r_C|$ . A small reflectivity is thus compensated by the large energy variation of  $\partial \Phi_{\text{tot}}/\partial \varepsilon$  close to the vacuum level. In particular for the resonance energy, the calculated width of 0.3 eV is sufficiently small for the resonance to be resolved. The

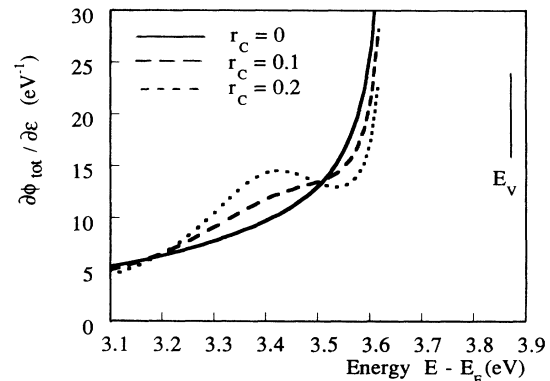


FIG. 2. Energy derivative of the total phase shift of the incoming electron wave at the surface of Al(111). This derivative is related to the surface-induced electron density of states. It is plotted vs energy for three different crystal reflectivities  $|r_C|$  where the curve with  $|r_C| = 0.1$  corresponds to the calculated value for Al(111). The resonance position is calculated to be at 0.47 eV below the vacuum level  $E_V$ . The energy scale is set to zero at the Fermi level and runs up to the vacuum level, indicated by the vertical bar, at 3.87 eV above the Fermi energy.

scattering amplitudes for the diffracted waves are less than  $|r_C| = 0.1$  at the considered scattering conditions which gives a justification to the neglect of diffracted waves in Eq. (1).

Comparing with experiments, we find that the calculated resonance position, at 0.47 eV below the vacuum level, is in good agreement with the observed surface-state energy, at 0.54 eV below the vacuum level, as measured by inverse photoemission.<sup>7</sup> The induced density of states, or the related quantity  $\partial\Phi_{\text{tot}}/\partial\varepsilon$ , cannot be immediately compared to observed intensities since it is not directly proportional to the intensity of emitted photons. In order to make some comparison of the calculated intensity to the experimentally observed one, we note that the absolute intensity of the resonance above the background, i.e.,  $\partial\Phi_B/\partial\varepsilon$  in Eq. (5), is about  $2 \text{ eV}^{-1}$ . This *absolute* strength is even higher than the strength of the resonance found in analogous calculations made for Na/Al(111) (Ref. 9) where the energies of the observed surface resonances were well reproduced.

When considering the presented model for image-state formation at other free-electron-like metals, we note that the crystal reflectivities of the most densely packed surfaces of Ba and Pb are at least as high as for Al(111) at an energy within an eV below their respective vacuum level.<sup>15</sup> Bearing in mind that the barrier potential from

which the electrons scatter is, in that energy region, more or less the image potential for these metals, there should be a good chance of observing similar resonant states on Ba(110) and Pb(111) as the one observed on Al(111). The conditions are the same; no band gap in an energy region close to the vacuum level but sufficient crystal reflectivity for an image state to form.

We conclude that electronic image-state formation at nearly-free-electron metals can be accounted for in a jellium description where the long-range part of the potential is corrected for the right imagelike behavior and the lattice effects are included via a pseudopotential description. Especially for Al(111), where a resonant state has been observed in an energy region with no metal band gap, we find that the lattice corrugation of the potential is able to provide the required crystal reflectivity for the formation of an image state in this region. The resolution of similar resonant states is also plausible on other free-electron-like metals, such as Ba and Pb.

It is a pleasure to thank S.-Å. Lindgren and L. Walldén for bringing this problem to our attention and, together with B. I. Lundqvist, for many stimulating discussions. Financial support from the Swedish Natural Science Research Council and the Swedish Board for Technical Developments is gratefully acknowledged.

<sup>1</sup>N. V. Smith, Rep. Prog. Phys. **51**, 1227 (1988).

<sup>2</sup>*Photoemission and the Electronic Properties of Surfaces*, edited by B. Feuerbacher, B. Fitton, and R. F. Willis (Wiley, New York, 1978).

<sup>3</sup>A. Zangwill, *Physics at Surfaces* (Cambridge Univ. Press, Cambridge, England, 1988).

<sup>4</sup>E. G. McRae, Rev. Mod. Phys. **51**, 541 (1979).

<sup>5</sup>G. V. Hansson and S. A. Flodström, Phys. Rev. B **18**, 1562 (1978).

<sup>6</sup>E. Caruthers, L. Kleinman, and G. P. Alldredge, Phys. Rev. B **8**, 4570 (1973).

<sup>7</sup>D. Heskett, K.-H. Frank, E. E. Koch, and H.-J. Freund, Phys. Rev. B **36**, 1276 (1987).

<sup>8</sup>S. Å. Lindgren and L. Walldén, Phys. Rev. B **38**, 10044

(1988).

<sup>9</sup>L.-A. Salmi and M. Persson, Phys. Rev. B **39**, 6249 (1989).

<sup>10</sup>P. M. Echenique and J. B. Pendry, J. Phys. C **11**, 2065 (1978).

<sup>11</sup>D. C. Wallace, Phys. Rev. **187**, 991 (1969).

<sup>12</sup>G. Paasch and H. Wonn, Phys. Status Solidi (b) **70**, 555 (1975).

<sup>13</sup>P. J. Jennings, R. O. Jones, and M. Weinert, Phys. Rev. B **37**, 6113 (1988).

<sup>14</sup>S. Å. Lindgren and L. Walldén, Phys. Rev. B **40**, 11546 (1989).

<sup>15</sup>The pseudopotentials for Ba and Pb were taken from a calculation by Heine and Animalu in W. A. Harrison, *Pseudopotentials in the Theory of Metals* (Benjamin, New York, 1966).